Review

Israel Journal of Chemistry

DOI: 10.1002/ijch.201900145

Macromolecular Superstructures: A Future Beyond Single Chain Nanoparticles

Hendrik Frisch,[a] Bryan T. Tuten,[a] and Christopher Barner-Kowollik*[a, b]

Abstract: Over the last 100 years polymer chemistry has flourished in all areas and enabled control over synthetic polymer architectures – including chain lengths, dispersity and monomer sequences. Compared to the architectures of biomacromolecules, these scientific achievements mainly took place on the level of primary structures. The plethora of functions carried out by proteins in nature, however, does not only result from their primary structure, but from its folding into perfectly defined 3D structures. Striving towards a similar architectural control and function in synthetic polymers, the field of single chain nanoparticles (SCNPs) emerged. In this review, we analyze the state of the art and identify what is currently standing between polymer chemistry and perfectly controlled synthetic macromolecular architectures. Based on the current challenges in the field of SCNPs, we discuss potential avenues to break today's barriers and explore future applications reaching beyond the current-state-of-the-art.

Keywords: single chain nanoparticles · polymer chemistry · macromolecular architectures · polymer ligations · polymerization reactions

1. Introduction

Ever since the pioneering work of Staudinger,[1] the perpetual quest towards control over macromolecular architectures has been fascinating and driven generations of chemists. Most of today's highly established fields of controlled macromolecular architectures including block copolymers, dendrimers and star polymers rest on the increasing control that we can exert over the primary structures of synthetic polymers. However, an orthogonal level of control over the architecture of polymers remained largely unexplored: the intramolecular crosslinking of single polymer chains.

While the first example dates back to the early 1960s,[2] polymer chemists began to crosslink single polymer chains. Inspired by the plethora of functions that are enabled by the perfect 3D arrangement of polypeptide chains in proteins, the field of single chain nanoparticles (SCNPs) emerged. Aiming to mimic the function of proteins, yet utilizing the synthetic ease of man-made polymers, SCNPs have the potential to overcome limitations of proteins with regard to scope and solvent for applications.[3–9] Combining toolboxes of organic, inorganic and polymer chemistry, a multitude of strategies has been successfully implemented for the intramolecular crosslinking of synthetic polymers.[10] The intramolecular crosslinks span covalent bonds, hydrogen bonds, host-guest interactions and coordinative bonds. Herein, we will refer to the intramolecular crosslinking of single polymer chains as 'folding' – inspired by the process that gives rise to their natural paragons, *i.e.* proteins.

Despite the progress within this thriving field, SCNPs remain far behind their natural paragons in regard to both complexity of the macromolecular architectures and resulting function. While SCNPs have been successfully applied as catalytic nanoreactors, mimicking the activity and selectivity of enzymes, catalysis is merely a single facet of these biomacromolecules. These perfectly arranged macromolecular architectures of proteins can *e.g.* perform macroscopic movement, storage, multiplication and read out of data as well as sensing. Yet, what is standing between polymer chemistry and this almost limitless potential? Herein, we critically explore the hurdles and challenges in the field of polymer chemistry limiting SCNP design and reflect on current strategies along with prospective avenues to overcome them in the future.

2. Synthesis: Tackling the Scalability

To initiate the intrachain crosslinking of single polymer chains, a wide variety of chemical reactions has been developed over the last decade, which were discussed in significant detail in reviews and books.[8,10] The extensive toolbox of reactions allows for versatile synthetic access, a high tolerance of functional groups and even orthogonal folding conditions for

[a] *H. Frisch, B. T. Tuten, C. Barner-Kowollik*
Centre for Materials Science, School of Chemistry and Physics
Queensland University of Technology (QUT)
2 George Street, Brisbane, QLD 4000 (Australia)
E-mail: christopher.barnerkowollik@qut.edu.au
[b] *C. Barner-Kowollik*
Macromolecular Architectures
Institut für Technische Chemie und Polymerchemie KarlsruheInstitute of Technology (KIT)
Engesserstr.18, 76131 Karlsruhe (Germany)

multi-step folding reactions.[11–14] Large scale synthesis of SCNPs, which is paramount for future applications, remains elusive despite the great variety of folding chemistries. The largest hurdle in the scale-up of SCNP synthesis is currently the highly dilute concentrations of the intramolecular cross-linking, which prevent the development of strategies to produce SCNPs beyond the gram scale. As the desired intrachain reaction competes with the parasitic interchain reaction, concentrations $< 1\ mg\,mL^{-1}$ are the current standard to achieve a selectivity for the intramolecular folding.[15] Some examples require even lower concentrations of $0.02\ mg\,mL^{-1}$,[14,16] $0.03\ mg\,mL^{-1}$[17] or $0.04\ mg\,mL^{-1}$.[18] Such low concentrations do not only drastically limit the scalability of SCNP synthesis, yet critically impede the online monitoring of the reactions – paramount towards improving our understanding of the folding process. For instance, nuclear magnetic resonance (NMR) spectroscopic methods would be an ideal tool to follow the reaction on the molecular level through 1D NMR and concomitantly on the macromolecular level, monitoring the folding of the chain *via* its reduction in its hydrodynamic diameter *via* diffusion ordered NMR techniques (DOSY). In the typically applied concentration regimes, however, these methods can practically not operate. As a consequence, characterization with NMR techniques is usually carried out after a purification and concentration step, subsequent to the folding reaction. Current strategies aiming to minimize the parasitic interchain reaction approach this challenge from multiple directions, including (i) experimental conditions (ii) polymer architecture, (iii) folding reaction and (iv) the polymerization of the main chain itself (Figure 1).

2.1 Experimental Conditions – Continuous Addition

A strategy that has proven to be efficient in scaling up SCNP synthesis relies on the continuous addition of a concentrated precursor polymer into a reactive solution. (Figure 1, top left**)**. If the polymer is added slower then it reacts, the effective low concentration of reactive polymer is maintained, while the concentration of unreactive SCNP increases continuously throughout the reaction. The continuous addition strategy was pioneered by the group of Hawker based on the dimerization of pendant *o*-quinodimethane moieties.[19] A concentrated solution of polymers containing benzocyclobutene was slowly added into benzyl ether at 250 °C. In the hot solvent, the benzocyclobutene groups isomerize into reactive *o*-quinodimethane species, which rapidly dimerize intramolecularly and induce the SCNP folding. Through the continuous addition of the precursor polymer, intermolecular reactions were suppressed and final SCNP concentrations of $2.5\ mg\,mL^{-1}$ were

Hendrik Frisch received his BSc (2010) and MSc (2012) in Chemistry from the University of Münster. He completed his PhD in 2016 under the supervision of Prof. Pol Besenius at the Organic Chemistry Institutes of the Universities of Münster and Mainz. In 2017 he joined the Queensland University of Technology (QUT) as a research fellow of the German national academy of sciences working together with Prof. Barner-Kowollik. In 2019 Hendrik received a Discovery Early Career Researcher Award from the Australian Research Council funding his research program on the development of synthetic polymer-peptide hybrid materials.

Bryan Tuten received his B.Sc. in Materials Chemistry at West Virginia Wesleyan College (USA, 2010). He then moved to the University of New Hampshire (USA) where he received his Ph.D.in Materials Science and Engineering (January 2016) under the supervision of Prof Erik Berda where he investigated the design and synthesis of single-chain polymer nanoparticles (SCNPs). Subsequently, he completed a one year postdoctoral research fellowship under the supervision of Prof Christopher Barner-Kowollik at the Karlsruhe Institute of Technology (Germany) and three years at Queensland University of Technology (Australia). Currently, Bryan is an Australian Research Council DECRA Fellow at QUT, focusing on the synergistic combination of chalcogen-based chemistry with macromolecular architecture.

Christopher Barner-Kowollik received his PhD in 1999 from Göttingen University. In 2006 he was appointed Full Professor of Polymer Chemistry at the Centre for Advanced Macromolecular Design at the University of New South Wales in Sydney. In 2008 he became chair for Macromolecular Chemistry at the Karlsruhe Institute of Technology (KIT) and is currently chair for Materials Chemistry at the Queensland University of Technology (QUT). In 2016, he was awarded the Erwin-Schroedinger Award of the Helmholtz Association (jointly with M. Wegener and M. Bastmeyer), in 2017 a Laureate Fellowship by the Australian Research Council (ARC) and most recently the 2020 UK Macro Medal. Christopher Barner-Kowollik is a Fellow of the Australian Academy of Science.

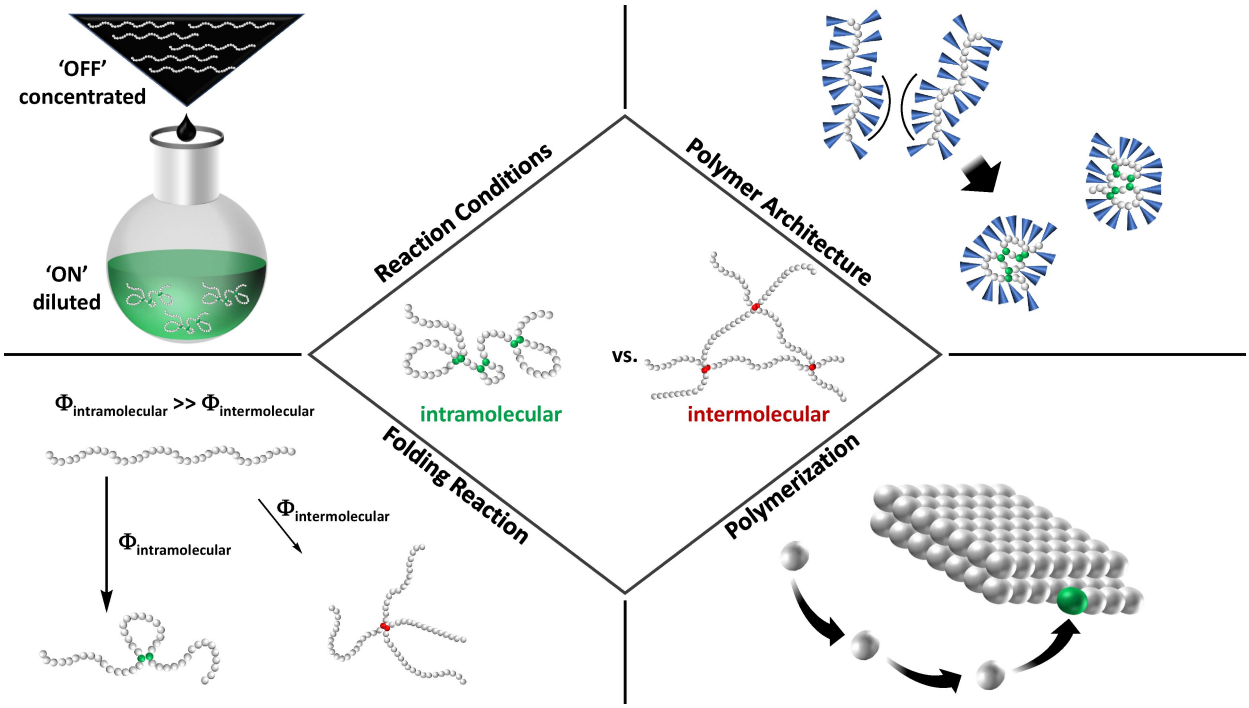

Figure 1. The efficient scale-up of SCNP synthesis is traditionally limited by ultra-diluted reaction conditions, resulting from the competition between the intramolecular and intermolecular crosslinking reaction. Current strategies applied to achieve a selectivity of intramolecular single chain folding over unwanted interchain reactions aim at the reaction conditions through a continuous addition approach (top left), the polymer architecture shielding the reactive groups (top right), the specific folding reaction by utilizing different quantum yield for intramolecular and intermolecular reaction (bottom left) and the polymerization reaction itself by combining a living polymerization with an immediate crystallization of the growing chain (bottom right).

obtained. To decrease the harsh reaction temperatures, the group of Harth investigated low temperature processes to generate the reactive o-quinodimethane unit.[20] Based on a benzocyclobutene alcohol derivative it was possible to reduce the required reaction temperature by 100 °C.[21] The Berda team combined the continuous addition strategy with the atom transfer radical coupling (ATRC) of pendent alkyl or benzyl bromide moieties on methacrylate-based polymers. The use of ATRC allowed for even milder reaction conditions at 80 °C and yielded SCNP concentrations of up to 10 mg mL^{-1} on the gram scale.[22]

While the previous examples investigate chain internal crosslinking of pendant reactive groups, various synthetic strategies of SCNP synthesis employ external crosslinkers. The reaction of these usually bivalent linkers is inherently different to the chain internal crosslinking, as it proceeds through two stages: (i) The intermolecular reaction between linker and precursor polymer and (ii) the intrachain reaction between the monovalently bound crosslinker and a complementary binding site in the polymer. Consequently, both reactions are likely to have different reactions rates, with the initial intermolecular reaction being the rate determining step.[23] Even at stoichiometric concentrations of reactive sites of the polymer and crosslinker, the concentration of crosslinker within the volume of the polymer coil will be understochociometric. Overstoichiometric amounts of crosslinkers can, thus, facilitate to achieve the maximum intramolecular crosslinking.[24] To investigate such effects of stoichiometry, the group of Berda investigated the effect of different crosslinkers equivalents of a bis-maleimide cross-linker on the folding of a polymer containing furane side chains.[25] Increasing equivalents of crosslinker lead to a more pronounced compaction of the SCNP, with 9 equivalents required to achieve the maximum compaction.

Taking the effects of an excess of crosslinker to the extreme, the discussed continuous addition strategy was also successfully applied to SCNP folding mediated by an external crosslinker. In this case, the parent polymer is slowly added to a solution containing the bivalent crosslinker. Successful examples of the continuous addition approach in external crosslinker mediated SCNP folding include reactions of isocyanates with amine crosslinkers to form urea linkages,[26] metal complexation of M_2^{4+} paddlewheel folding motifs,[27] photochemical crosslinking[28] and Thiol-Michael additions.[29] The continuous addition procedure, thus, presents a versatile route for both external and internal crosslinker mediated folding, to suppress the parasitic interchain reaction and achieve an efficient scale up of SCNP synthesis.

2.2 Polymer Architecture – Shielding of the Reactive Sites

Orthogonally to the crosslinking chemistry, the choice of polymer backbone has shown to drastically influence the competition between intra- and intermolecular reaction (Figure 1, top right). The group of Qiao reported single chain folding of random copolymers of oligo(ethylene glycol) methyl etheracrylate, di(ethylene glycol) ethyl ether acrylate and 4-(acryloyloxy)-ε-caprolactone at unprecedented concentrations of 100 mg mL^{-1} in chloroform.[30] When the same folding chemistry, *i.e.* the ring opening polymerization of the pendant caprolactone units, was applied to poly(styrene) or poly(methyl acrylate) based polymers instead of the sterically demanding poly(oligo(ethylene glycol) acrylate based polymers, the unwanted interchain reaction became predominant.[31] The brush like structure of the oligoethylene glycole sidechain appears to sterically shield the folding reaction from interchain reactions. As a consequence, also entirely different folding chemistries utilizing non-covalent interactions such as hydrophobic interactions[32] and the hydrogen bonded BTA motive[33] have reported comparably high folding concentrations, if applied to poly(oligo(ethylene glycol) methacrylate based polymers (up to 60 and 100 mg mL^{-1}).

The concept of shielding macromolecular architectures was recently extended by the group of Zimmerman, designing a stepwise process of initial hydrophobic collapse followed by intramolecular covalent crosslinking.[34] When the precursor polyacrylamide polymer with pendant decyltrimethylammonium and azidopropyl sidechains was added to water, unimolecular micelles were formed. The hydrophobic core could subsequently be crosslinked with a hydrophobic crosslinker diyne using the CuAAC reaction at concentrations near 100 fold higher than previously reported covalent folding of the same group.[35] The combination of intramolecular compartmentalization and electrostatic shielding of the reactive hydrophobic compartment, thus suppresses the intermolecular reaction that is reported to occur in CuAAC mediated SCNP folding even at contraction < 0.05 mg mL^{-1}.[12] The concept of electrostatic shielding was further extended by the group of Yang based on PVP-containing polymers, PAA-contained polymers, and PI-contained polymers, achieving an intramolecular crosslinking in concentrated solution of up to 300 mg mL^{-1}.[36]

2.3 Selectivity of the Crosslinking Reaction

The above discussed sterical shielding limits the architectural freedom of the SCNP and the subsequent addition approach utilizes low concentrations of reactive species, which prevent the on-line monitoring of the folding reaction. Thus, a crosslinking chemistry that has an inherent preference for the intramolecular reactions would be highly desirable. While most of the above folding reactions are thermally driven, photochemical reactions hold the potential to overcome the requirements of high dilutions. In the photochemical folding of SCNPs, the crosslinking reaction has to compete with radiative and non-radiative relaxation pathways. If an excited molecule does not find a suitable reaction partner within the lifetime of its excited state, the molecule is deactivated and not reactive anymore. Consequently, the quantum yield (φ) of the photoreaction is diffusion and concentration dependent – and occurs only above a certain concentration threshold (Figure 1, bottom left).[37,38] Since the concentration of photoreactive units within the polymer coil is higher than the global concentration of photoreactive units in the reaction vessel, the quantum yield of the intramolecular reaction is significantly higher than for intermolecular pathway.

Using the [2+2] photocycloaddition chemistry of a stilbene derivative, styrylpyrene, we have recently reported a quantum yield of $\varphi = 0.07$ for the intrachain dimerization of a polymer containing 28% of pendant reactive units.[37] When the same photoreactive molecule was investigated in free solution, without macromolecular confinement at the same overall concentration (0.7 mM), the quantum yield was observed to be close to zero and no reaction could be detected. Even when increasing the concentration of the non-polymer bound species by a factor of 14 (10 mM), the quantum yield was still significantly lower than within the macromolecular confinement ($\varphi = 0.02$). The selectivity for the intrachain reaction can be further increased by not deoxygenating the folding reaction, as O_2 acts as a triplet state quencher and reduces the lifetimes of the triplet states, which is critical for the diffusion controlled intermolecular reaction. Based on the confinement effect on the photoreaction, folding reactions up to 25 mg mL^{-1} were enabled.

Note that such a strategy only applies to photochemical reactions such as [2+2] and [4+4] cycloadditions.[39] Reactions using thermally reactive intermediates, which are photochemically generated, generally have lifetimes too long to effect the described selectivity. Reaction of such photo caged intermediates such as nitrile imines,[40] thioaldehydes and *o*-quinodimethanes[41] suffer from the previously noted ultradilute conditions in the range of 0.01 mg mL^{-1}.

2.4 Polymerization: In situ Polymerization and Folding

As outlined above, the synthesis of SCNPs is generally carried out in two steps: Synthesis of the precursor polymer, followed by single chain folding. The group of Mecking recently challenged this paradigm by developing a synthetic approach that enabled the direct folding of growing polymer chains (Figure 1, bottom right and Figure).[42] Based on a living aqueous catalytic polymerization, a long-lived water-stable Ni (II) catalyst initiated the polymerization of ethylene, whereas immediate crystallization of the growing chain in water initiated its folding. Resulting from a highly effective nucleation of the polymer crystallization, each growing single polymer chain crystal comprised only one active site. Both the single polymer chains and the resulting nanocrystal grow in a

living fashion. Based on this strategy, extremely high SCNP concentrations of up to 13 wt-% could be achieved.

3. Architecture Beyond Intramolecular Crosslinks

A particularly attractive feature of SCNPs lies in their unique architecture. SCNPs are unique from other polymeric nanoobjects in that they have crosslinked nanodomains, setting them apart from other polymeric nanoobjects such as macrocycles (folded object with no chain termini), dendrimers (non-folded object with a dense core and many chain termini), and (hyper)branched polymers (non-folded object without a dense core and many chain termini). By precisely understanding and controlling these internal crosslinks, the macromolecular architecture of these nanoobjects can be finely controlled.

3.1 Secondary Structure Inspired Order of Subdomains

Based on significant progress in precision polymer chemistry, synthetic control over chain lengths[43–47] and monomer sequences[48–51] has been largely achieved and enabled the synthesis of uniform sequence defined polymers.[52–54] Compared to the levels of protein structures – the natural inspiration of SCNPs – the current state-of-the-art allows controlling the primary structure, *i.e.* monomer sequence, of the linear polymer precursor reasonably well. The tertiary, or external structure, of SCNPs i. e. ellipsoids, spheres, loosely folded, densely folded, etc, is also relatively well controlled, utilizing the previously outlined toolbox of folding chemistries. However, a critical gap lies in the precise control of the internal secondary structure of SCNPs, accessing highly ordered 3D local chain segments.

3.1.1 Incorporating Defined Domains into SCNPs

Initial steps have been undertaken in this endeavor such as the work of the Berda team, who synthesized porphyrin-cored nanoparticles (PCPNs) as heme iron protein models (Figure 2). By carefully designing a four-armed polymer with a heme moiety embedded within a hydrophobic core, these authors were able to demonstrate that the PCPNs could be used as synthetic analogues towards native systems with both redox chemistry as well as ligand-binding reactivity.[55] Further developments from the Berda laboratory include the use of both Passerini and Ugi chemistries to generate dipeptide based crosslinks. Further, these authors were able to incorporate a small level of secondary structure by creating an internal domain by introducing internal α-hydrazino turns based on the sequential folding of hydrazone motifs. Although these internal α-hydrazino turns were unable to affect change of the SCNP's tertiary structure, this still marks a critical step towards the design of the *internal* space of SCNPs.[56] Significant progress within the realm of internally defined

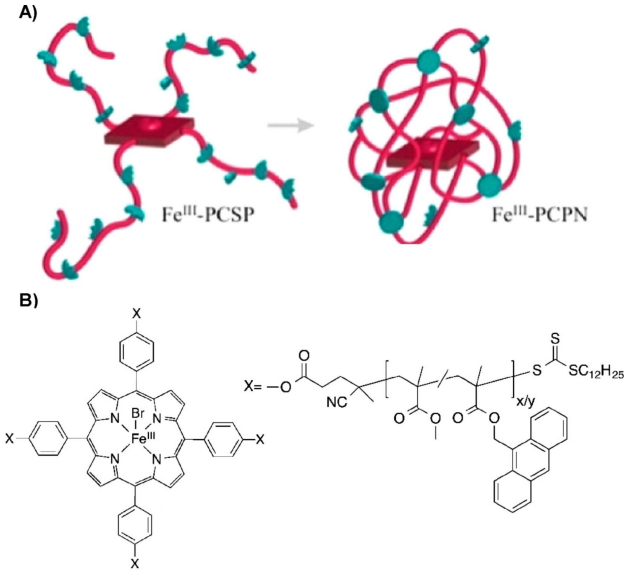

Figure 2. A) Schematic representation of the photoinduced folding of porphyrin-cored star polymers (PCSP) into a porphyrin-cored polymer nanoparticle (PCPN) upon anthracene dimerization. B) Chemical structure of the parent PCSP.[58] Adapted with permission from *Inorg. Chem.* 2016, 55, 19, 9493–9496. Copyright 2016 American Chemical Society.

domains in SCNPs has also been made by the Meijer team. A broad array of complex macromolecular architectures have been folded by the utilization of benzene-1,3,5-tricarboxamide (BTA) motifs. These moieties, when exposed to water, form elongated helical stacks via a 3-fold hydrogen bonds. Further, the helicity of these internal domains can be tuned based on the chirality of the alkyl side chains of the BTA units.[57] These complex internal domains have further been used to design a broad array of SCNPs, which are catalytically active in water.[58–61]

3.1.2 Encoding Secondary Structure into Synthetic Polymers

To equip synthetic polymers or oligomers with a secondary structure that either mimics or fully adopts the same structural motifs observed in nature (including helices, sheets and coils), the field of foldamers emerged.[62] The critical conformational preference that defines the foldamer results from the design of its monomeric units, which can be based on natural[63] or non-natural building blocks.[64]

Pioneering work of Huck, for instance, developed oligomers that mimic beta-sheet based architectures – not based on hydrogen bonds, but aromatic interactions.[65,66] Moving from oligomers relying on iterative synthesis to polymers, the group of Weck, developed a remarkable toolbox of monomers that induce secondary structures in synthetic polymer strands (Figure 3). To mimic sheet like architectures, rigid poly(*p*-phenylene vinylene) species (PPVs) have been employed,

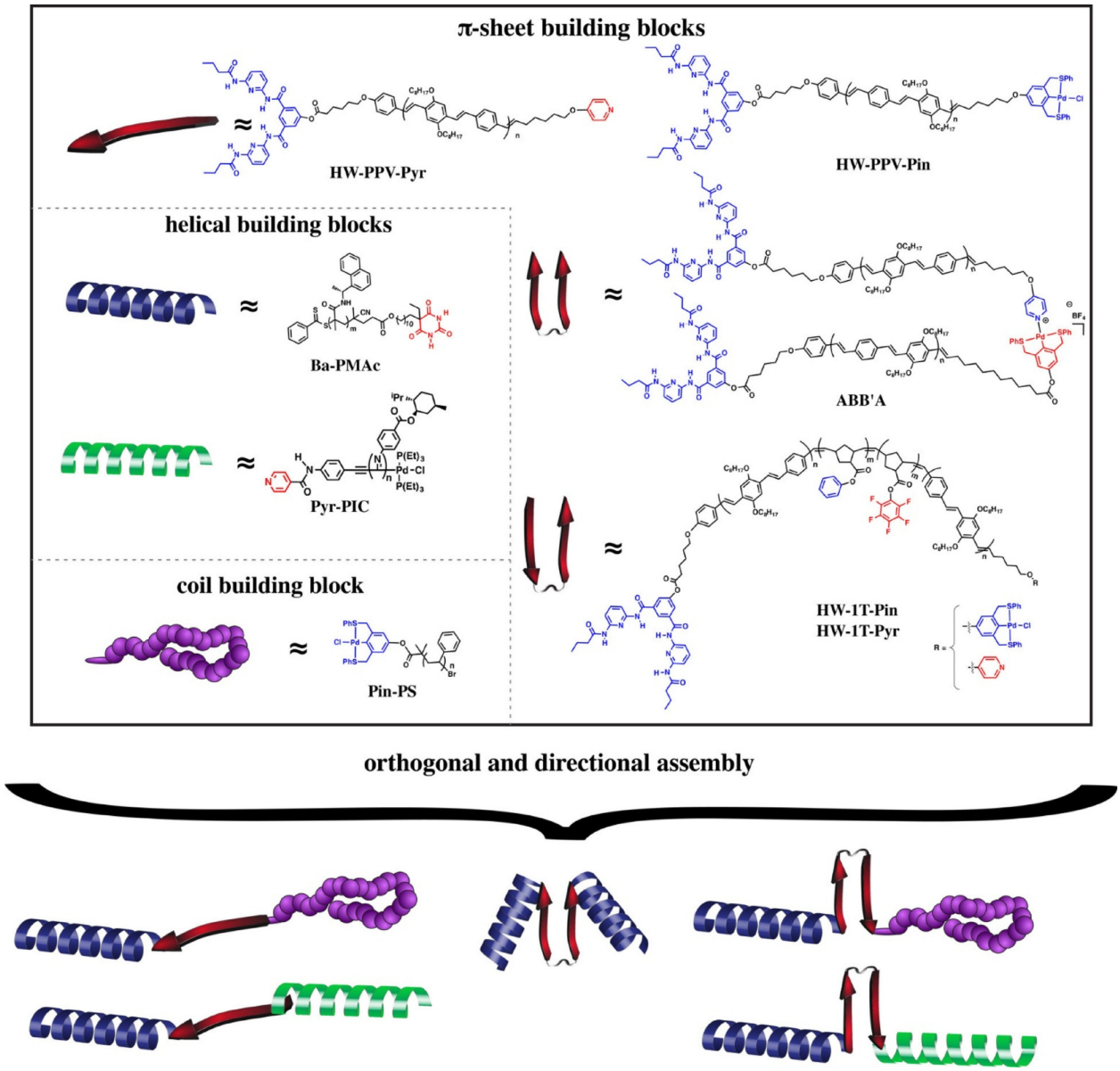

Figure 3. Schematic Representation of the Target Supramolecular Block Copolymers Comprising π-Sheets, Helices, and Coils via a Plug-and-Play Strategy Utilizing Orthogonal Metal Coordination and Hydrogen Bonding.[69] Reprinted with permission from (*J. Am. Chem. Soc. 2017, 139, 35, 12240–12250*). Copyright 2019 American Chemical Society.

which can be synthetically accessed via living ring-opening metathesis polymerization (ROMP) of substituted [2.2]paracyclophane-1,9-dienes (pCpd).[67–71] In addition to the rigidity of the conjugated polymer backbone, the PPV strands allow to monitor their face-to-face π-π stacking through fluorescence quenching upon assembly of the strands.[69] Approaching the conformation of beta-sheets observed in nature even further, strategies were developed to direct the arrangement of multiple strands in an either parallel or anti-parallel fashion.[69] The parallel arrangement was achieved by end-functionalization of the ROMP polymers through the addition of termination agents containing complementary recognition motifs for self-assembly. Upon self-assembly both strands are supramolecularly linked at the same chain end, yielding the parallel conformation. Anti-parallel sheet assembly was achieved by synthesizing block copolymers featuring a sheet-coil-sheet architecture. The middle segment is thereby designed to promote a beta-turn like folding of the two flanking PPV blocks. Synthetically, those architectures are accessible through an iterative living ROMP: after the sheet forming pCpd is polymerized to completion, norbonenes containing phenyl and pentafluorophenyl sidechains are added to form the coil block. The entire synthetic cycle was successfully repeated multiple times, yielding polymers of up 16 blocks.[71]

To achieve helical conformations of polymer strands, poly (methacrylamide)s and poly(isocyanide)s, have both proven to be effective, whereby the helical handness can be induced by chiral sidechains.[68,72,73] For instance, right handed helical conformation can be obtained through a palladium catalyzed polymerization of menthol-based phenyl isocyanide monomers. Following a macroinitiation strategy that combines palladium-mediated isocyanide polymerization with ROMP, block copolymers comprising covalently linked helical and sheet like conformations can be readily obtained.[70] The synthetic accessibility of such helical polymer segments was recently further extended through the development of heterotechelic helical poly(methacrylamide) (PMAc).[74] The orthogonal supramolecular binding sites of both chain termini enabled the selective attachment of polymer blocks comprising different secondary structures on either side of the helical block.

Merging such far reaching control over polymer segment conformation with covalent single chain folding reactions would enable an unprecedented level of architectural control of SCNPs. Especially the synergy between crosslinking reaction and structural conformation of chain segments is highly appealing to break into new ground – much closer to the architectural sophistication of architectures found in nature.

With only limited work in this area, there is key potential for important and fascinating discoveries. Establishing the ability to not only control the primary and tertiary structures, yet the secondary structures would immediately open the door to design and implement synthetic enzymes with the potential to catalyze any number of biologically or industrially important reactions.

3.1.3 Introducing Order in SCNP through Crystalline Structures

As highlighted in the synthesis section, using crystalline order in SCNPs has critical, yet largely untapped potential. In addition to the high concentrations, which are accessible through the strategy of in-situ polymerization and crystallization driven folding, the highly distinct internal order can translate into defined anisotropic macromolecular architecture (Figure 4).[42] The preferred deposition of the growing polymer chain onto the {110} crystalline growth front gave rise to uniform and monodisperse particles, whose shape evolved from truncated lozenges to lozenges over the course of the SCNP growth.

We feel that an appropriate analogy can be drawn from the plethora of fascinating discoveries within the metal-organic framework (MOF) field, whereby precisely controlled, three dimensional nanoobjects have led to some incredible structure/property relationships which include breakthroughs in hydrogen storage,[75] selective heterogeneous catalysis,[76] regulating channels for polymerizations,[77] and selective carbon dioxide capture[78] just to name a few. Furthermore, by attaining control over all three levels of structural control, work could immediately begin on higher order, multi-tiered structures. Just as in their counterparts in Nature, precisely folded polymers which are then able to precisely assemble, will lead to an entirely new field within polymer and materials science. Although the precise three-dimensional structure of MOFs has yet to be duplicated using exclusively soft matter materials (i.e. without the need of a metal atom), elegant work at fusing the fields of polymer science and MOFs into polyMOFs has been undertaken by the Johnson team.[79–81]

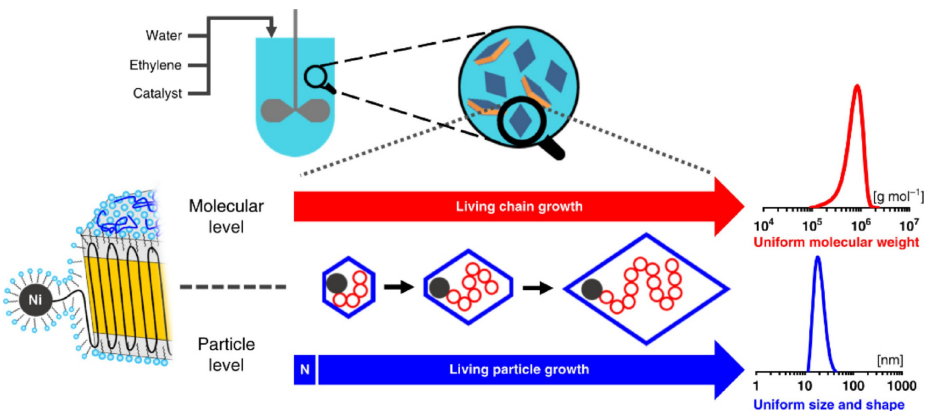

Figure 4. Concept to obtain uniform size and shape particles by controlled polymerization on a molecular as well as particle level. An effective nucleation (N) ensures that particles contain only one active site, and start to grow virtually at the same time. Due to the living character of polymerization, all particles continue to grow for the entire duration of the experiment, to yield particles each composed of a chain of identical length. As the growing chains are immediately deposited on the growing single-crystal particle during this process, particle shape evolves uniformly over time during polymerization.[41] Reproduced with permission from *Nat Commun* 10, 2592 (2019). Copyright © 2019, Springer Nature.

3.2 Towards Quaternary SCNP Structures

Regarding different levels of architectural control, we have discussed monomer sequences (primary structure), polymer strand conformations (secondary structure) and the intramolecular crosslinking of single polymer chains into SCNPs (tertiary structure). However, taking further inspiration from nature, the architecture of a large number of proteins emerges from the perfect arrangement of multiple ordered peptide strands into a quaternary structure.

To assemble multiple SCNPs into a super structure, pioneering approaches are based on the self-assembly of amphiphilic tadpole structured SCNPs, containing a folded block and linear block.[82] The group of Perrier used reversible boronate ester chemistry to crosslink diblock copolymers consisting of 4-acryloylmorpholine and glycerol acrylate (Figure 5).[83] The resulting tadpole SCNPs self-assembled into spherical multimeric structures. Upon lowering the pH or addition of sugar, the boronic ester based crosslinking of the glycerol block was reversed, which induced the disassembly of the SCNP superstructure.

As the ratio between the hydrophilic and hydrophobic block controls the morphology of polymer assemblies,[84,85] an understanding of the structure-size relationship of tadpole

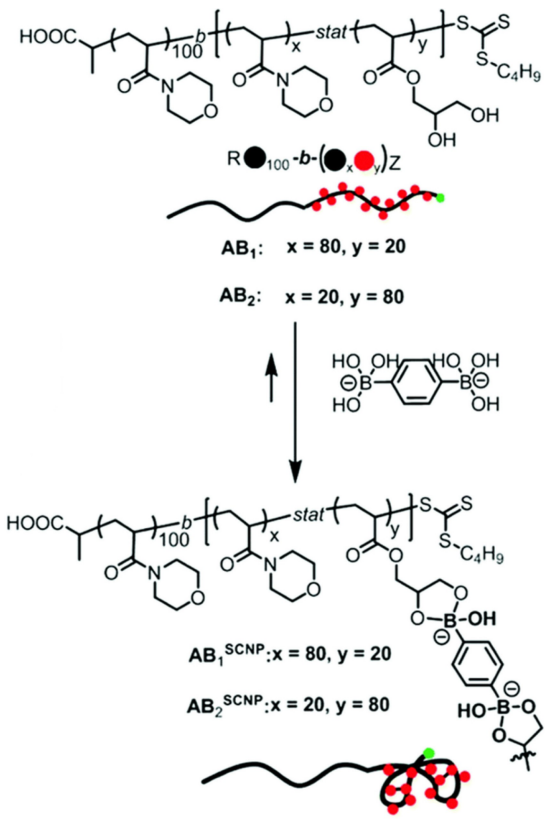

Figure 5. Schematic representation of the synthesis of tadpole-like SCNPs.[78] Reproduced from Ref. [78] with permission from the Royal Society of Chemistry.

SCNPs is highly valuable. Taking into account the hydrodynamic radius of the parent polymer, the number fraction of monomers of both blocks and the number of formed crosslinks in the SCNP block, the group of Pomposo developed structure-size relationships for an *a priori* SCNP design.[86] The critical effect of the folding degree of tadpole SCNPs on their self-assembly was recently evidenced by the group of He.[17] Amphiphilic diblock copolymers of poly(*N*,*N*′-dimethylacrylamide)-*block*-polystyrene (PDMA-*b*-PS) with photocrosslinkable cinnamoyl groups in one of the two blocks, enabled the folding of either the hydrophilic or hydrophobic block. In both blocks, increasing degrees of folding induced a morphological transition of the self-assembled architecture, as a result from the changed hydrophobic to hydrophilic balance upon intramolecular crosslinking. A full phase diagram, elucidating the interplay of intrachain crosslinking degree and mass fraction of the linear blocks was recently established by the group of Chen (Figure 6).[87] By varying the irradiation time of the photo crosslinking and the lengths of the hydrophilic block, a library of different morphologies including vesicles, spheres, tubes, lamellae, doughnuts, and connected spheres was obtained, providing architectural guidelines on how the design of SCNPs controls their self-assembly. In addition to the degree of folding, the modulation of the charge density of the folded block has shown to affect the morphologies of SCNP assemblies.[88]

More complex SCNPs, comprising two different polymer blocks that are both folded were recently reported.[89] The resulting single chain Janus particles were found to assemble into lamellar structures. Remarkably, the self-assembly of the SCNPs could also be utilized for their purification after the folding reactions of both blocks. Since the inclusion of both less folded and intramolecularly crosslinked SCNPs into the self-assembled structures is energetically unfavored, the macromolecular assemblies contained exclusively homogeneous Janus SCNPs. Separation from the supernatant suspension, thus, provided a straight forward purification of Janus shaped SCNPs.

As outlined above, self-assembly is a viable strategy to construct higher order architectures consisting of multiple polymer strands. While the architecture of the SCNP building blocks has successfully enabled a certain degree of control over the morphology of the resulting self-assembly, individual events of intrachain association cannot be controlled using this avenue. In order to obtain remote control over single chain folding and intrachain association, orthogonal chemistries that allow to trigger exclusively one of the two reactions are key. In addition to the spatiotemporal control of photochemical reactions, different wavelengths of light hold the potential to initiate the reaction of selected molecules based on their absorption. However, most molecules display absorption overlaps at shorter wavelengths. Reactions can therefore only be initiated selectively in a defined sequence from longer to shorter wavelengths, since the lower wavelengths would initiate both reactions simultaneously. To overcome this limitation, we developed a strategy that utilized photorever-

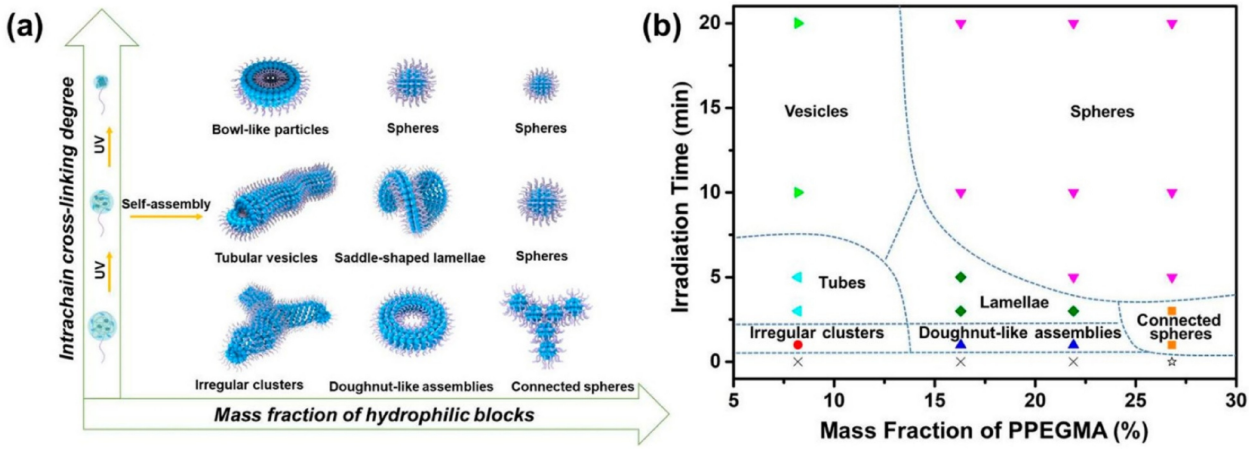

Figure 6. (a) Schematic illustration for the self-assembly of liquid crystalline single chain Janus nanoparticles (LC-SCJNPs) with various cross-linking degree and hydrophilic/hydrophobic block ratios in selective solvent. (b) Phase diagram of assemblies for various mass fraction of PPEGMA in PPEGMA-*b*-PMAStb with various irradiation time. (☆) represent assemblies with irregular morphology, and (×) represent precipitation.[87] Reprinted with permission from (*Macromolecules* 2019, 52, 8, 2956–2964). Copyright 2019 American Chemical Society.

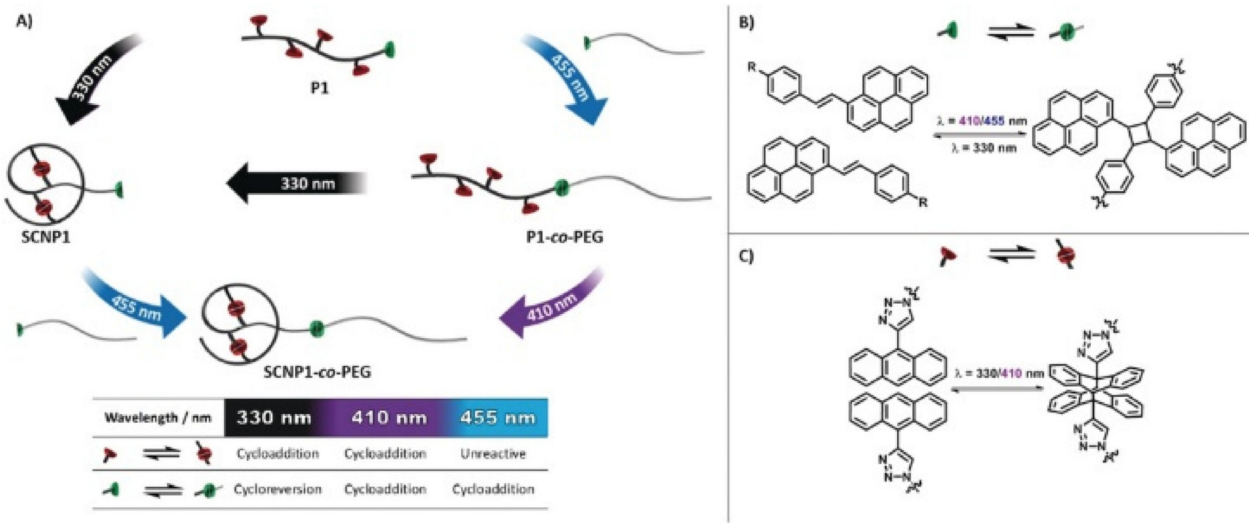

Figure 7. Schematic representation of the light-induced intrachain crosslinking and single-chain ligation pathways of P1 (A). The dual photoreactive parent polymer P1 can be ligated with a PEG chain through the [2+2] cycloaddition of styrylpyrene (B) and folded into an SCNP through the [4+4] cycloaddition of 9-triazolylanthracene units distributed along the backbone (C). Since the 9-triazolylanthracene dimerization can only be initiated by irradiation at $\lambda = 330$ and 410 nm, while the styrylpyrene dimerization can be initiated at $\lambda = 410$ and 455 nm and reverted at $\lambda = 330$ nm, selective triggering of the two dimerization reactions becomes accessible: Initial irradiation at $\lambda = 330$ nm suppresses the reaction of the terminal photoreactive group, yet initiates the SCNP folding. The obtained SCNP1 can subsequently be ligated with a second polymer chain also a containing terminal styrylpyrene unit to form SCNP1-*co*-PEG at $\lambda = 455$ nm. The same macromolecular architecture can be obtained in the reverse order, by initial ligation of P1 at $\lambda = 455$ nm to P1-*co*-PEG and subsequent folding of the photoreactive block at $\lambda = 410$ nm to SCNP1-*co*-PEG.[85] Reprinted with permission from Ref. [85] copyright 2010 Wiley-VCH.

sible [2+2] cycloadditions as the longer wavelength reactive species to suppress the unwanted reaction at shorter wavelengths (Figure 7). By incorporating a styrylpyrene unit at the chain end and pendant 9-triazolylanthracene units as the lower wavelength reactive species along the back bone, a dual photoreactive polymer was obtained. As a consequence, it is now possible to either trigger the reaction of the pendant anthracene units to induce the SCNP folding, or the interchain association through the terminal styrylpyrene. Importantly both reactions could be triggered subsequently and in any given order, only depending on the color of light.[90]

The developed concept of sequence independent orthogonal ligation chemistry was readily applied to generate spatially resolved polymer coatings from a single multi material

photoresists.[91] The transfer from single chain technology into materials applications exemplifies how chemistry developed in SCNPs can be translated into applications of soft matter materials.

4. Analysis Beyond Compaction of the Hydrodynamic Volume

One of the fundamental challenges within the field of SCNPs is the accurate analysis of the *internal* structure. Almost all of the analytical techniques at the polymer chemist's disposal can only "see" the tertiary, or external, structure, as evident in the classic means for confirming the successful synthesis of an SCNP, i.e. size-exclusion chromatography (SEC), or more broadly, any technique that is used to measure the pervated volume of the SCNP in a given solution. Typically, with SEC as the analytical method, a shift to longer retention times, indicating a smaller, more compact polymer is indication of SCNP formation. Similarly, Barner-Kowollik and coworkers, through a careful review of the literature, have demonstrated that methods utilizing the intrinsic viscosity via the Stokes-Einstein equation such as viscometry and 2D diffusion ordered spectroscopy (DOSY) NMR are particularly accurate when considering the range of possible densities of SCNPs.[92] Recently, we outlined many of the ongoing challenges in the characterization of SCNPS.[93] Currently, light scattering techniques remain a challenge with analyzing SCNPs. First, there is the physical limitation that most SCNPs have a hydrodynamic diameter less than 10 nm which thereby makes them anisotropic scatterers of light, rendering their morphology invisible to these techniques. Furthermore, Barner-Kowollik and team have also compiled a broad sampling of the literature in regards to dynamic light scattering (DLS) and have shown that there seems to be no observable correlation between hydrodynamic radius and the possible ranges of density of a polymeric object (Figure 8).[92] Initial studies from Pomposo and coworkers have begun to use small angle neutron scattering (SANS) techniques to overcome many of the difficulties associated with standard scattering techniques.[94,95]

Developing analytical techniques which are capable of accurately assessing the inner structure of SCNPs will be critical for the future of the field. By being able to more accurately analyze the internal structure of these nanoobjects, more advanced strategies can be employed for precisely tailoring internal SCNP structure. Currently, this is relatively unexplored territory within the SCNP field. Only limited examples, to date, have shown effective at analyzing the internal SCNP crosslinking structure such as the SEC-ESI-MS technique employed for both chain-[96] and step-growth[97] polymers. This methodology offers the polymer architect a powerful tool in determining the number of crosslinks, the nature of the crosslinks (i.e. a propagation-based crosslinking or a bimolecular coupling based crosslinking). Currently, the

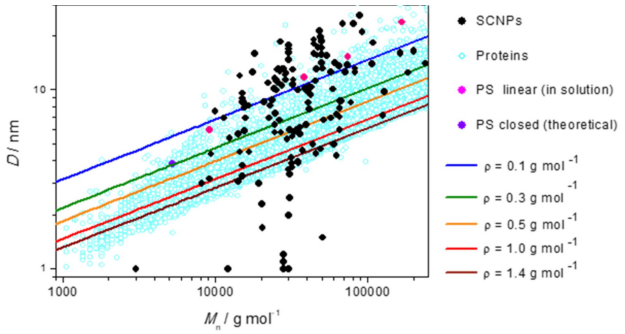

Figure 8. D vs. (apparent) M_n of the literature reported SCNPs, as well as calculated D_h values of 37 000 different proteins (light blue circles), linear polystyrene in a good solvent (pink dots) and theoretically calculated D_h for 5 kDa polystyrene in a closed conformation (violet dot).[87] Reproduced from Ref. [87] with permission from the Royal Society of Chemistry.

predominant disadvantage of this analytical methodology is the extensive expertise and data processing times, although advances in ESI-MS software for complex peak analysis and assignment have begun development.[98] Other techniques employed in order to gain in-depth understanding of the inner workings of SCNPs also include the excellent work from the Gormley team where small angle x-ray scattering (SAXS) was used to elucidate both compactness and chain flexibility within a comprehensive library of various SCNPs synthesized from homopolymers, random heteropolymers, block copolymers, PEG-conjugated polymers, and other polymer functionalized SCNPs.[99] Other interesting and 'non-traditional' approaches to the mapping of the internal structures of SCNPs include the size-scaling analysis coupled to TEM imaging to map the internal local domains within SCNPs by the Pomposo team.[100] In addition, the Meijer team has demonstrated that the force-driven mechanical unfolding of SCNPs via single-molecule force spectroscopy (SMFS) provides information regarding the internally crosslinked domains.[101]

With only these limited techniques available to the polymer architect, it becomes clear that further development into analytical methods of SCNPs is needed. Useful metrics to understand when designing and creating SCNPs are variables such as the internal Kuhn length of both the crosslinks as well as the folded polymer backbone. Modifying the techniques for analyzing branching density to apply to the internal cross-linking of SCNPs would also be invaluable information to have readily on hand. With just these two variables, an internal three dimensional image can start to be constructed from direct analytical data instead of having to rely heavily on advanced MD modelling such as the excellent work out of the Sommer lab.[102] With the knowledge of how various backbones and crosslinking chemistries behave when folded, the polymer architect can begin to design polymers which will fold in a predictable manor, allowing for tailor made internal structures suited to specific properties and functions.

5. Function beyond Catalytic Nanoreactors

The unrivalled reaction control of enzymes is without a doubt a major driver in the field of SCNPs. Consequently, the application of SCNPs as catalytic nanoreactors is arguably the most advanced in the field[34,103–106] and thoroughly discussed in recent reviews.[107,108] Given the plethora of functions displayed by proteins – SCNPs' natural counterparts – there exists a vastly untapped field of functions beyond just catalysis. A particularly intriguing task of proteins is to gate movement. Ranging from the intracellular transport in cells[109] to macroscopic movements of muscles,[110] most movements in biology are enabled by motor proteins. Different classes of motor proteins have different task fields, structures, and modes of motion. One thing the different classes of proteins have in common, is that movement results from a small conformation change of the motor domain the ATP hydrolysis cycle. Great efforts have been made to create synthetic walking molecules[111] and molecular machines[112] able to conduct and mimic such movements. Such approaches are still missing in the field of SCNPs.

A major hurdle in the development of SCNPs that can conduct movement, is that reversible conformational changes are surprisingly scarce in SCNPs. Compared to the sophistication of nature, even the simple reversible conformational change of folding and unfolding is only sparsely investigated. Existing systems enabling a controlled folding and unfolding are mostly limited to non-covalent chemistries. Examples include a stepwise and order-independent unfolding, where hydrogen bonds and host-guest interactions were reversed upon addition of methanol or competing guest molecules pioneered by Barner-Kowollik and Luy.[113] Using temperature or single molecular force spectroscopy, the group of Meijer has investigated the unfolding hydrogen bonded BTA based SCNPs.[101] Regarding covalent SCNP folding, disulfide bonds were used to fold and unfold SCNPs upon reduction or oxidation.[114] A common disadvantage of these existing systems is their dependence on chemical and physical stimuli, which have a limited spatiotemporal control. In contrast, light enables facile access to precise spatiotemporal control. A very promising light gated tool to control covalent bond formations are photoreversible photocycloadditions.[39] Irradiation of one wavelength induces thereby a [2+2] or [4+4] cycloaddition between two molecules to induce their ligation. As the resulting cycloadduct formation comes along with a reduction of the conjugated system, a shorter wavelength is required to excite the photoproduct and reverse its formation. Consequently, these reactions are generally investigated for intermolecular reactions and executed in such a way that one wavelength induces bond formation, while a shorter one reverses it. However, none of the SCNP systems reported until today enabled the expected unfolding upon cycloreversion at shorter wavelengths.[37,115,116] While the bond forming cycloaddition is highly attractive for SCNP folding as outlined in the synthesis section, is the cycloreversion strongly suppressed by the confined environment within the polymer coil. Wavelength dependent photoreactivity studies within SCNPs showed that the bond forming photocycloaddition reaction, which is commonly suppressed in the lower wavelength regime in case of intermolecular reactions, becomes predominant over the entire investigated wavelength regime.[37] The observed drastic change of reactivity can be explained by altered reaction kinetics within SCNPs. Both the photoreactive alkene and cycloadduct absorb light and can be excited in the lower wavelength regime. In the case of an intermolecular reaction the monomolecular cycloreversion is kinetically strongly favored, whereas the macromolecular confinement within SCNPs forces the split molecules to remain in close proximity, which kinetically favors the cycloaddition reaction to the point where both reactions have reaction rates in the same order of magnitude.

While light gated folding and unfolding of SCNPs remains unachieved until today, the groups of Barner-Kowollik and Lehn recently developed a strategy to remotely control conformations of SCNPs with light.[117] Acyclic diene metathesis (ADMET) polymerization of *N*-alkyl α-bisimine dienes enabled the synthesis of polymer containing dual reactive moieties embedded into their backbones. The imine containing polymer could be folded into an SCNP upon addition metal ions inducing metal-ligand interactions. Orthogonally, the conformation was controlled upon light induced isomerization of the backbone incorporated imines. The study not only highlights the potential to control conformations of SCNPs, yet also the potential that lies within functional polymer backbones.

In addition to light, mechanical fields are a trigger that enables high temporal control through immediate responses of the material. The group of Diesendruck recently reported a fascinating example of mechanically triggered SCNP unfolding (Figure 9).[15] Based on the transition metal-π interaction induced folding developed in the laboratory of Lemcoff,[118–120] poly(butadienes) containing additional mechanophores where folded upon addition of rhodium(I)-ethylene complexes. When mechanical stress is applied via sonication, it was transferred from the backbone to the weaker intramolecular Rh_2Cl_2-π crosslinks resulting in an unfolding of the SCNP. Since the Rh-π bonds form spontaneously, the developed strategy also enables an intramolecular repairing mechanism that allows to reform bonds within the SCNP after enduring mechanical stress. A process that is inspired by biomaterials observed in nature, where proteins absorb mechanical stress through a defined scission of intramolecular crosslinks and reform upon release of stress.[121] This creative work thus not only enables remote control over SCNP folding and unfolding, but also points out the vast potential SCNPs have in materials applications.

While individual SCNPs are highly promising for imaging[122] and targeting[123] applications in biological systems, bulk properties of their ensembles are barley investigated. The possibility to direct mechanical energy from the polymer main chain onto the internal crosslinks of SCNPs provides one example how SCNPs could be used to tailor

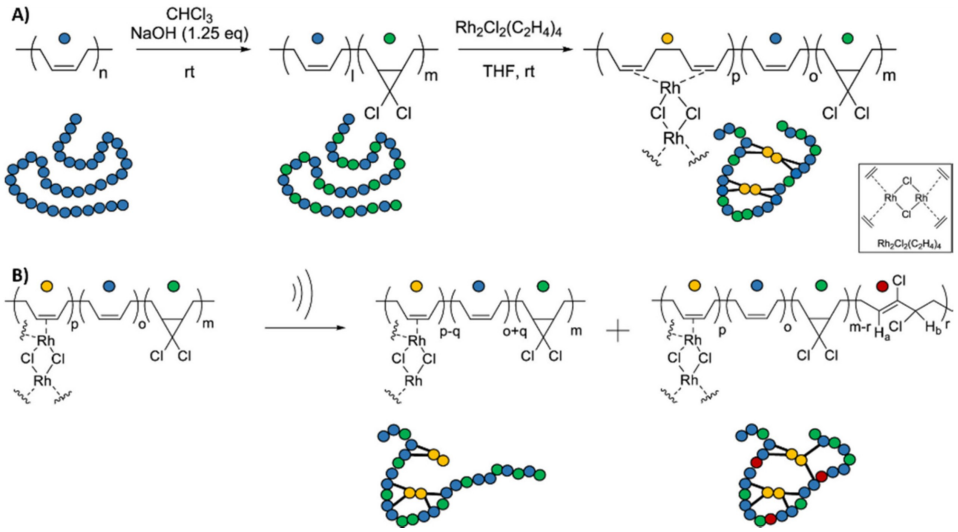

Figure 9. A) SCNP folding based on rhodium-π-bond coordination. SCNPs were obtained by treating linear polybutadiene (PB) with a rhodium (I)-ethylene complex in high dilution, where the ethylene ligands are substituted by the double bonds in the polymer backbone. An advantage to using PB is that it allows the incorporation of gem-dichlorocyclopropane (gem-DCC) mechanophores to the backbone B) Nonchain scissile mechanochemical events of folded polymer during sonication.[15] Reprinted with permission from (*J. Am. Chem. Soc. 2019, 141, 18, 7256–7260*). Copyright 2019 American Chemical Society.

future soft matter materials with unprecedented functions emerging from their SCNP building blocks.

6. Summary and Outlook

The field of single chain nanoparticles has experienced rapid growth since it renaissance during the last one and a half decades. SCNP technology holds the potential to transform specific application fields, most prominently the field of bioinspired catalysis. Herein, we have shown that precision macromolecular chemistry in conjunction with covalently and non-covalently driven folding motifs allows to selectively fold and unfold SCNPs. However, the nature of the folding is – expect a select few examples – chaotic and far removed from the natural paragons on which SCNPs are modelled. In our view, it is thus the next critical step to enable control over the folding process itself, so that specific sub-geometries of SCNPs can be selectively folded and unfolded to close and open specific pockets within their core. Ideally, such geometric reconfigurations should be remotely controlled, best by finely energy and intensity gated colors of light, opening the possibility to selectively open and close catalytic pockets. Our vision thus entails catalytically active metallo-SCNPs, whose catalytic activity can be switched on and off remotely by light. The chemistry shown herein gives promising leads to reach such an ambitious goal, yet it is also evident that no technology exists that would allow a spatially resolved reconfiguration of SCNP structures within their core. We hope that the current perspective will spur efforts in reaching the above goal.

Acknowledgements

H.F., B.T.T. and C.B.-K. acknowledge continued support from the Queensland University of Technology (QUT) through the Centre for Materials Science. H.F. and B.T.T. acknowledge support by the Australian Research Council (ARC) in the form of DECRA Fellowships and C.B.-K. in the form of a Laureate Fellowship enabling his photochemical research program. C. B–K. additionally acknowledges support by the Karlsruhe Institute of Technology in the context of the STN program of the Helmholtz association.

References

[1] H. Staudinger, *Ber. Dtsch. Chem. Ges.* **1920**, *53*, 1073–1085.
[2] W. Kuhn, G. Balmer, *J. Polym. Sci.* **1962**, *57*, 311–319.
[3] D. Mecerreyes, V. Lee, C. J. Hawker, J. L. Hedrick, A. Wursch, W. Volksen, T. Magbitang, E. Huang, R. D. Miller, *Adv. Mater.* **2001**, *13*, 204–208.
[4] M. Seo, B. J. Beck, J. M. J. Paulusse, C. J. Hawker, S. Y. Kim, *Macromolecules* **2008**, *41*, 6413–6418.
[5] E. J. Foster, E. B. Berda, E. W. Meijer, *J. Am. Chem. Soc.* **2009**, *131*, 6964–6966.
[6] T. Terashima, T. Mes, T. F. A. De Greef, M. A. J. Gillissen, P. Besenius, A. R. A. Palmans, E. W. Meijer, *J. Am. Chem. Soc.* **2011**, *133*, 4742–4745.
[7] C. K. Lyon, A. Prasher, A. M. Hanlon, B. T. Tuten, C. A. Tooley, P. G. Frank, E. B. Berda, *Polym. Chem.* **2015**, *6*, 181–197.
[8] J. Pomposo, *Single-Chain Polymer Nanoparticles: Synthesis, Characterization, Simulations, and Applications*, Wiley-VCH, Weinheim, Germany, **2017**.

[9] A. M. Hanlon, C. K. Lyon, E. B. Berda, *Macromolecules* **2016**, *49*, 2–14.
[10] S. Mavila, O. Eivgi, I. Berkovich, N. G. Lemcoff, *Chem. Rev.* **2016**, *116*, 878–961.
[11] T. Mes, R. van der Weegen, A. R. A. Palmans, E. W. Meijer, *Angew. Chem. Int. Ed. Engl.* **2011**, *50*, 5085–9.
[12] J. Rubio-Cervilla, H. Frisch, C. Barner-Kowollik, J. A. Pomposo, *Macromol. Rapid Commun.* **2019**, *40*, 1800491.
[13] H. Frisch, D. Kodura, F. R. Bloesser, L. Michalek, C. Barner-Kowollik, *Macromol. Rapid Commun.* **2019**, *0*, 1900414.
[14] I. Dashan, D. K. Balta, B. A. Temel, G. Temel, *Macromol. Chem. Phys.* **2019**, *220*, 1900116.
[15] A. Levy, R. Feinstein, C. E. Diesendruck, *J. Am. Chem. Soc.* **2019**, *141*, 7256–7260.
[16] J. T. Offenloch, E. Blasco, S. Bastian, C. Barner-Kowollik, H. Mutlu, *Polym. Chem.* **2019**, *10*, 4513–4518.
[17] S. Thanneeru, W. Li, J. He, *Langmuir* **2019**, *35*, 2619–2629.
[18] T. S. Fischer, S. Spann, Q. An, B. Luy, M. Tsotsalas, J. P. Blinco, H. Mutlu, C. Barner-Kowollik, *Chem. Sci.* **2018**, *9*, 4696–4702.
[19] E. Harth, B. Van Horn, V. Y. Lee, D. S. Germack, C. P. Gonzales, R. D. Miller, C. J. Hawker, *J. Am. Chem. Soc.* **2002**, *124*, 8653–8660.
[20] T. A. Croce, S. K. Hamilton, M. L. Chen, H. Muchalski, E. Harth, *Macromolecules* **2007**, *40*, 6028–6031.
[21] J. N. Dobish, S. K. Hamilton, E. Harth, *Polym. Chem.* **2012**, *3*, 857.
[22] A. M. Hanlon, R. Chen, K. J. Rodriguez, C. Willis, J. G. Dickinson, M. Cashman, E. B. Berda, *Macromolecules* **2017**, *50*, 2996–3003.
[23] R. Li, B. J. McCoy, *Macromol. Rapid Commun.* **2004**, *25*, 1059–1063.
[24] C. K. Lyon, E. O. Hill, E. B. Berda, *Macromol. Chem. Phys.* **2016**, *217*, 501–508.
[25] A. M. Hanlon, I. Martin, E. R. Bright, J. Chouinard, K. J. Rodriguez, G. E. Patenotte, E. B. Berda, *Polym. Chem.* **2017**, *8*, 5120–5128.
[26] J. B. Beck, K. L. Killops, T. Kang, K. Sivanandan, A. Bayles, M. E. Mackay, K. L. Wooley, C. J. Hawker, *Macromolecules* **2009**, *42*, 5629–5635.
[27] N. D. Knöfel, H. Rothfuss, C. Barner-Kowollik, P. W. Roesky, *Polym. Chem.* **2019**, *10*, 86–93.
[28] I. Dashan, D. K. Balta, B. A. Temel, G. Temel, *Eur. Polym. J.* **2019**, *113*, 183–191.
[29] A. P. P. Kröger, N. M. Hamelmann, A. Juan, S. Lindhoud, J. M. J. Paulusse, *ACS Appl. Mater. Interfaces* **2018**, *10*, 30946–30951.
[30] E. H. H. Wong, S. J. Lam, E. Nam, G. G. Qiao, *ACS Macro Lett.* **2014**, *3*, 524–528.
[31] E. H. H. Wong, G. G. Qiao, *Macromolecules* **2015**, *48*, 1371–1379.
[32] T. Terashima, T. Sugita, K. Fukae, M. Sawamoto, *Macromolecules* **2014**, *47*, 589–600.
[33] P. J. M. Stals, M. A. J. Gillissen, T. F. E. Paffen, T. F. A. de Greef, P. Lindner, E. W. Meijer, A. R. A. Palmans, I. K. Voets, *Macromolecules* **2014**, *47*, 2947–2954.
[34] J. Chen, J. Wang, K. Li, Y. Wang, M. Gruebele, A. L. Ferguson, S. C. Zimmerman, *J. Am. Chem. Soc.* **2019**, *141*, 9693–9700.
[35] Y. Bai, H. Xing, G. A. Vincil, J. Lee, E. J. Henderson, Y. Lu, N. G. Lemcoff, S. C. Zimmerman, *Chem. Sci.* **2014**, *5*, 2862–2868.
[36] X. Dao, C. Xi, T. Lin, J. Bingyin, Y. Zhenzhong, *CCS Chem.* **2020**, *1*, 407–430.
[37] H. Frisch, J. P. Menzel, F. R. Bloesser, D. E. Marschner, K. Mundsinger, C. Barner-Kowollik, *J. Am. Chem. Soc.* **2018**, *140*, 9551–9557.
[38] O. A. Fedorova, A. E. Saifutiarova, E. N. Gulakova, E. O. Guskova, T. M. Aliyeu, N. E. Shepel, Y. V. Fedorov, *Photochem. Photobiol. Sci.* **2019**, *18*, 2208–2215.
[39] H. Frisch, D. E. Marschner, A. S. Goldmann, C. Barner-Kowollik, *Angew. Chem. Int. Ed.* **2018**, *57*, 2036–2045; *Angew. Chem.* **2018**, *130*, 2054–2064.
[40] T. Nitsche, J. Steinkoenig, K. De Bruycker, F. R. Bloesser, S. J. Blanksby, J. P. Blinco, C. Barner-Kowollik, *Macromolecules* **2019**, *52*, 2597–2606.
[41] T. K. Claus, J. Zhang, L. Martin, M. Hartlieb, H. Mutlu, S. Perrier, G. Delaittre, C. Barner-Kowollik, *Macromol. Rapid Commun.* **2017**, *38*, 1700264.
[42] M. Schnitte, A. Staiger, L. A. Casper, S. Mecking, *Nat. Commun.* **2019**, *10*, 2592.
[43] M. Szwarc, *Nature* **1956**, *178*, 1168–1169.
[44] G. Moad, E. Rizzardo, S. H. Thang, *Polymer (Guildf).* **2008**, *49*, 1079–1131.
[45] M. Kamigaito, T. Ando, M. Sawamoto, *Chem. Rev.* **2001**, *101*, 3689–3746.
[46] C. J. Hawker, A. W. Bosman, E. Harth, *Chem. Rev.* **2001**, *101*, 3661–3688.
[47] K. Matyjaszewski, J. Xia, *Chem. Rev.* **2001**, *101*, 2921–2990.
[48] J.-F. Lutz, M. Ouchi, D. R. Liu, M. Sawamoto, *Science (80-.).* **2013**, *341*, 628.
[49] J.-F. Lutz, *Polym. Chem.* **2010**, *1*, 55.
[50] M. Ouchi, N. Badi, J.-F. Lutz, M. Sawamoto, *Nat. Chem.* **2011**, *3*, 917–924.
[51] N. G. Engelis, A. Anastasaki, R. Whitfield, G. R. Jones, E. Liarou, V. Nikolaou, G. Nurumbetov, D. M. Haddleton, *Macromolecules* **2018**, *51*, 336–342.
[52] R. B. Merrifield, *J. Am. Chem. Soc.* **1963**, *85*, 2149.
[53] M. A. R. Meier, C. Barner-Kowollik, *Adv. Mater.* **2019**, *31*, 1806027.
[54] J. O. Holloway, K. S. Wetzel, S. Martens, F. E. Du Prez, M. A. R. Meier, *Polym. Chem.* **2019**, *10*, 3859–3867.
[55] K. J. Rodriguez, A. M. Hanlon, C. K. Lyon, J. P. Cole, B. T. Tuten, C. A. Tooley, E. B. Berda, S. Pazicni, *Inorg. Chem.* **2016**, *55*, 9493–9496.
[56] J. P. Cole, J. J. Lessard, K. J. Rodriguez, A. M. Hanlon, E. K. Reville, J. P. Mancinelli, E. B. Berda, *Polym. Chem.* **2017**, *8*, 5829–5835.
[57] O. Altintas, M. Artar, G. ter Huurne, I. K. Voets, A. R. A. Palmans, C. Barner-Kowollik, E. W. Meijer, *Macromolecules* **2015**, *48*, 8921–8932.
[58] Y. Liu, P. Turunen, B. F. M. de Waal, K. G. Blank, A. E. Rowan, A. R. A. Palmans, E. W. Meijer, *Mol. Syst. Des. Eng.* **2018**, *3*, 609–618.
[59] Y. Liu, S. Pujals, P. J. M. Stals, T. Paulöhrl, S. I. Presolski, E. W. Meijer, L. Albertazzi, A. R. A. Palmans, *J. Am. Chem. Soc.* **2018**, *140*, 3423–3433.
[60] M. Artar, A. R. A. Palmans, **2017**, pp. 105–123.
[61] P. J. M. Stals, C.-Y. Cheng, L. van Beek, A. C. Wauters, A. R. A. Palmans, S. Han, E. W. Meijer, *Chem. Sci.* **2016**, *7*, 2011–2015.
[62] S. Hecht, I. Huc, *Foldamers: Structure, Properties and Applications*, Wiley-VCH, Weinheim, **2007**.
[63] T. A. Martinek, F. Fülöp, *Chem. Soc. Rev.* **2012**, *41*, 687–702.
[64] G. Guichard, I. Huc, *Chem. Commun.* **2011**, *47*, 5933–5941.
[65] L. Sebaoun, V. Maurizot, T. Granier, B. Kauffmann, I. Huc, *J. Am. Chem. Soc.* **2014**, *136*, 2168–2174.

[66] L. Sebaoun, B. Kauffmann, T. Delclos, V. Maurizot, I. Huc, *Org. Lett.* **2014**, *16*, 2326–2329.
[67] E. Elacqua, M. Weck, *Chem. Eur. J.* **2015**, *21*, 7151–7158.
[68] E. Elacqua, A. Croom, K. B. Manning, S. K. Pomarico, D. Lye, L. Young, M. Weck, *Angew. Chem. Int. Ed.* **2016**, *55*, 15873–15878; *Angew. Chem.* **2016**, *128*, 16105–16110.
[69] E. Elacqua, K. B. Manning, D. S. Lye, S. K. Pomarico, F. Morgia, M. Weck, *J. Am. Chem. Soc.* **2017**, *139*, 12240–12250.
[70] S. K. Pomarico, D. S. Lye, E. Elacqua, M. Weck, *Polym. Chem.* **2018**, *9*, 5655–5659.
[71] E. Elacqua, G. T. Geberth, D. A. Vanden Bout, M. Weck, *Chem. Sci.* **2019**, *10*, 2144–2152.
[72] A. Croom, K. B. Manning, M. Weck, *Macromolecules* **2016**, *49*, 7117–7128.
[73] F. Takei, K. Onitsuka, S. Takahashi, *Macromolecules* **2005**, *38*, 1513–1516.
[74] R. Deng, M. Milton, S. K. Pomarico, M. Weck, *Polym. Chem.* **2019**, *10*, 5087–5093.
[75] L. J. Murray, M. Dincă, J. R. Long, *Chem. Soc. Rev.* **2009**, *38*, 1294.
[76] J. Lee, O. K. Farha, J. Roberts, K. A. Scheidt, S. T. Nguyen, J. T. Hupp, *Chem. Soc. Rev.* **2009**, *38*, 1450.
[77] T. Uemura, N. Yanai, S. Kitagawa, *Chem. Soc. Rev.* **2009**, *38*, 1228.
[78] J.-R. Li, R. J. Kuppler, H.-C. Zhou, *Chem. Soc. Rev.* **2009**, *38*, 1477.
[79] Y. Wang, M. Zhong, J. V. Park, A. V. Zhukhovitskiy, W. Shi, J. A. Johnson, *J. Am. Chem. Soc.* **2016**, *138*, 10708–10715.
[80] Y. Gu, M. Huang, W. Zhang, M. A. Pearson, J. A. Johnson, *Angew. Chem. Int. Ed.* **2019**, *58*, 16676–16681.
[81] M. J. MacLeod, J. A. Johnson, *Polym. Chem.* **2017**, *8*, 4488–4493.
[82] F. Xu, Z. Fang, D. Yang, Y. Gao, H. Li, D. Chen, *ACS Appl. Mater. Interfaces* **2014**, *6*, 6717–6723.
[83] J. Zhang, J. Tanaka, P. Gurnani, P. Wilson, M. Hartlieb, S. Perrier, *Polym. Chem.* **2017**, *8*, 4079–4087.
[84] E. B. Zhulina, M. Adam, I. LaRue, S. S. Sheiko, M. Rubinstein, *Macromolecules* **2005**, *38*, 5330–5351.
[85] A. E. Smith, X. Xu, S. E. Kirkland-York, D. A. Savin, C. L. McCormick, *Macromolecules* **2010**, *43*, 1210–1217.
[86] I. Asenjo-Sanz, E. Verde-Sesto, J. A. Pomposo, *Phys. Chem. Chem. Phys.* **2019**, *21*, 10884–10887.
[87] W. Wen, T. Huang, S. Guan, Y. Zhao, A. Chen, *Macromolecules* **2019**, *52*, 2956–2964.
[88] J. Wen, J. Zhang, Y. Zhang, Y. Yang, H. Zhao, *Polym. Chem.* **2014**, *5*, 4032–4038.
[89] L. Jiang, M. Xie, J. Dou, H. Li, X. Huang, D. Chen, *ACS Macro Lett.* **2018**, *7*, 1278–1282.
[90] H. Frisch, F. R. Bloesser, C. Barner-Kowollik, *Angew. Chem. Int. Ed.* **2019**, *58*, 3604–3609.
[91] S. Bialas, L. Michalek, D. E. Marschner, T. Krappitz, M. Wegener, J. Blinco, E. Blasco, H. Frisch, C. Barner-Kowollik, *Adv. Mater.* **2019**, *31*, 1807288.
[92] E. Blasco, B. T. Tuten, H. Frisch, A. Lederer, C. Barner-Kowollik, *Polym. Chem.* **2017**, *8*, 5845–5851.
[93] J. Engelke, J. Brandt, C. Barner-Kowollik, A. Lederer, *Polym. Chem.* **2019**, *10*, 3410–3425.
[94] J. A. Pomposo, I. Perez-Baena, F. Lo Verso, A. J. Moreno, A. Arbe, J. Colmenero, *ACS Macro Lett.* **2014**, *3*, 767–772.
[95] A. Arbe, J. Rubio-Cervilla, A. Alegría, A. J. Moreno, J. A. Pomposo, B. Robles-Hernández, P. Malo de Molina, P. Fouquet, F. Juranyi, J. Colmenero, *Macromolecules* **2019**, *52*, 6935–6942.
[96] J. Steinkoenig, H. Rothfuss, A. Lauer, B. T. Tuten, C. Barner-Kowollik, *J. Am. Chem. Soc.* **2017**, *139*, 51–54.
[97] J. Steinkoenig, T. Nitsche, B. T. Tuten, C. Barner-Kowollik, *Macromolecules* **2018**, *51*, 3967–3974.
[98] K. De Bruycker, T. Krappitz, C. Barner-Kowollik, *ACS Macro Lett.* **2018**, *7*, 1443–1447.
[99] R. Upadhya, N. S. Murthy, C. L. Hoop, S. Kosuri, V. Nanda, J. Kohn, J. Baum, A. J. Gormley, *Macromolecules* **2019**, acs.macromol.9b01923.
[100] J. A. Pomposo, A. J. Moreno, A. Arbe, J. Colmenero, *ACS Omega* **2018**, *3*, 8648–8654.
[101] N. Hosono, A. M. Kushner, J. Chung, A. R. A. Palmans, Z. Guan, E. W. Meijer, *J. Am. Chem. Soc.* **2015**, *137*, 6880–6888.
[102] H. Rabbel, P. Breier, J.-U. Sommer, *Macromolecules* **2017**, *50*, 7410–7418.
[103] Y. Bai, X. Feng, H. Xing, Y. Xu, B. K. Kim, N. Baig, T. Zhou, A. A. Gewirth, Y. Lu, E. Oldfield, *J. Am. Chem. Soc.* **2016**, *138*, 11077–11080.
[104] J. Chen, J. Wang, Y. Bai, K. Li, E. S. Garcia, A. L. Ferguson, S. C. Zimmerman, *J. Am. Chem. Soc.* **2018**, *140*, 13695–13702.
[105] R. Lambert, A.-L. Wirotius, S. Garmendia, P. Berto, J. Vignolle, D. Taton, *Polym. Chem.* **2018**, *9*, 3199–3204.
[106] S. Garmendia, S. B. Lawrenson, M. C. Arno, R. K. O'Reilly, D. Taton, A. P. Dove, *Macromol. Rapid Commun.* **2019**, *40*, 1900071.
[107] H. Rothfuss, N. D. Knöfel, P. W. Roesky, C. Barner-Kowollik, *J. Am. Chem. Soc.* **2018**, *140*, 5875–5881.
[108] J. Rubio-Cervilla, E. González, J. A. Pomposo, *Nanomaterials* **2017**, *7*, 341.
[109] R. D. Vale, *Cell* **2003**, *112*, 467–480.
[110] T. A. Duke, *Proc. Natl. Acad. Sci. USA* **1999**, *96*, 2770–2775.
[111] M. von Delius, D. A. Leigh, *Chem. Soc. Rev.* **2011**, *40*, 3656–3676.
[112] S. Kassem, T. van Leeuwen, A. S. Lubbe, M. R. Wilson, B. L. Feringa, D. A. Leigh, *Chem. Soc. Rev.* **2017**, *46*, 2592–2621.
[113] T. S. Fischer, D. Schulze-Sünninghausen, B. Luy, O. Altintas, C. Barner-Kowollik, *Angew. Chem. Int. Ed.* **2016**, *55*, 11276–11280; *Angew. Chem.* **2016**, *128*, 11446–11450.
[114] B. Tuten, D. Chao, C. Lyon, E. B. Berda, *Polym. Chem.* **2012**.
[115] P. G. Frank, B. T. Tuten, A. Prasher, D. Chao, E. B. Berda, *Macromol. Rapid Commun.* **2014**, *35*, 249–253.
[116] J. He, L. Tremblay, S. Lacelle, Y. Zhao, *Soft Matter* **2011**, *7*, 2380–2386.
[117] L. Greb, H. Mutlu, C. Barner-Kowollik, J.-M. Lehn, *J. Am. Chem. Soc.* **2016**, *138*, 1142–1145.
[118] M. Sudheendran, D. C. E. L. Sivan, A. Liron, S. Rafi, L. N. Gabriel, *Angew. Chem. Int. Ed.* **2013**, *52*, 5767–5770; *Angew. Chem.* **2013**, *125*, 5879–5882.
[119] I. Berkovich, S. Mavila, O. Iliashevsky, S. Kozuch, N. G. Lemcoff, *Chem. Sci.* **2016**, *7*, 1773–1778.
[120] S. Mavila, I. Rozenberg, N. G. Lemcoff, *Chem. Sci.* **2014**, *5*, 4196–4203.
[121] M. Rief, *Science (80-.).* **1997**, *276*, 1109–1112.
[122] D. N. F. Bajj, M. V. Tran, H.-Y. Tsai, H. Kim, N. R. Paisley, W. R. Algar, Z. M. Hudson, *ACS Appl. Nano Mater.* **2019**, *2*, 898–909.
[123] A. P. P. Kröger, M. I. Komil, N. M. Hamelmann, A. Juan, M. H. Stenzel, J. M. J. Paulusse, *ACS Macro Lett.* **2019**, *8*, 95–101.

Manuscript received: November 15, 2019
Revised manuscript received: January 23, 2020
Version of record online: March 5, 2020